3-1-2023

# Apolipoprotein M attenuates anthracycline cardiotoxicity and lysosomal injury

Zhen Guo

Carla Valenzuela Ripoll

Antonino Picataggi

David R Rawnsley

Mualla Ozcan

*See next page for additional authors*

## Authors

Zhen Guo, Carla Valenzuela Ripoll, Antonino Picataggi, David R Rawnsley, Mualla Ozcan, Ezhilarasi Chendamarai, Amanda Girardi, Terrence Riehl, Hosannah Evie, Ahmed Diab, Attila Kovacs, Krzysztof Hyrc, Xiucui Ma, Lauren N Pedersen, Carmen Bergom, Nathan O Stitziel, Michael P Rettig, John F DiPersio, Abhinav Diwan, Ali Javaheri, and et al.

JACC: BASIC TO TRANSLATIONAL SCIENCE VOL. 8, NO. 3, 2023


ORIGINAL RESEARCH - PRECLINICAL

# Apolipoprotein M Attenuates Anthracycline Cardiotoxicity and Lysosomal Injury

Zhen Guo, PhD,[a] Carla Valenzuela Ripoll, MD,[a] Antonino Picataggi, BS,[a] David R. Rawnsley, MD, PhD,[a] Mualla Ozcan, MD,[a] Julio A. Chirinos, MD, PhD,[b] Ezhilarasi Chendamarai, PhD,[a] Amanda Girardi, BS,[a] Terrence Riehl, PhD,[a] Hosannah Evie, BS,[a] Ahmed Diab, MD,[a] Attila Kovacs, MD,[a] Krzysztof Hyrc, PhD,[c] Xiucui Ma, PhD,[a,d] Aarti Asnani, MD,[e] Swapnil V. Shewale, PhD,[b] Marielle Scherrer-Crosbie, MD, PhD,[b] Lauren Ashley Cowart, PhD,[f,g] John S. Parks, PhD,[h] Lei Zhao, MD, PhD,[i] David Gordon, PhD,[i] Francisco Ramirez-Valle, MD, PhD,[i] Kenneth B. Margulies, MD,[b] Thomas P. Cappola, MD,[b] Ankit A. Desai, MD,[j] Lauren N. Pedersen, PhD,[a] Carmen Bergom, MD, PhD,[a] Nathan O. Stitziel, MD, PhD,[a] Michael P. Rettig, PhD,[a] John F. DiPersio, MD, PhD,[a] Stefan Hajny, PhD,[k,l] Christina Christoffersen, MD, PhD,[k,l] Abhinav Diwan, MD,[a,d] Ali Javaheri, MD, PhD[a]

## VISUAL ABSTRACT

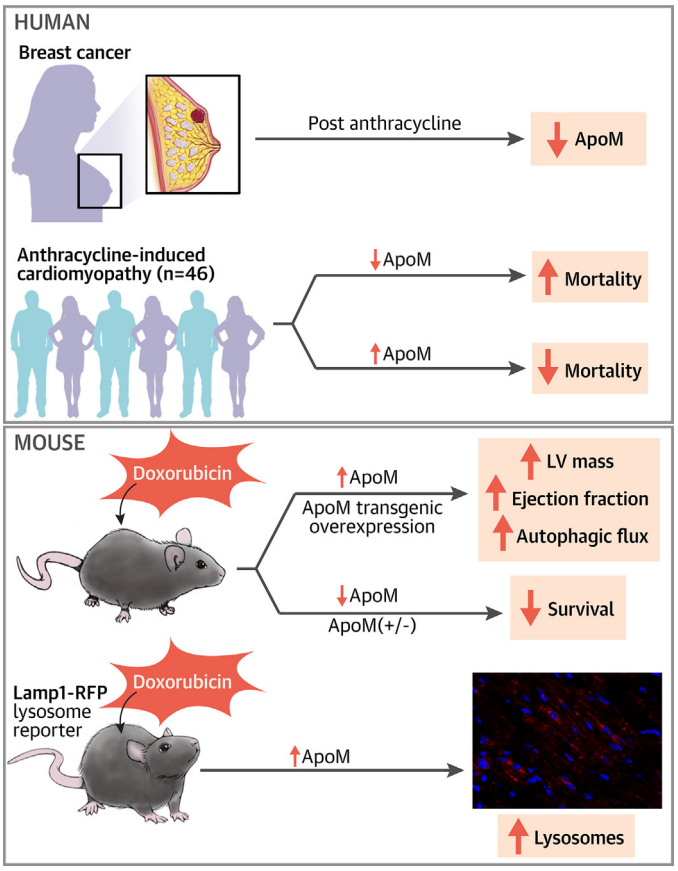


Guo Z, et al. J Am Coll Cardiol Basic Trans Science. 2023;8(3):340–355.

## HIGHLIGHTS

- **Circulating ApoM is inversely associated with mortality in human anthracycline-induced cardiomyopathy.**
- **Anthracycline treatment reduces circulating ApoM in humans and mice.**
- **Increasing ApoM attenuates doxorubicin cardiotoxicity and lysosomal injury and preserves myocardial autophagic flux, but it does not affect doxorubicin antineoplastic efficacy.**
- **Autophagic impairment is characteristic of human anthracycline cardiomyopathy.**

ISSN 2452-302X https://doi.org/10.1016/j.jacbts.2022.09.010

**SUMMARY**

Apolipoprotein M (ApoM) binds sphingosine-1-phosphate (S1P) and is inversely associated with mortality in human heart failure (HF). Here, we show that anthracyclines such as doxorubicin (Dox) reduce circulating ApoM in mice and humans, that ApoM is inversely associated with mortality in patients with anthracycline-induced heart failure, and ApoM heterozygosity in mice increases Dox-induced mortality. In the setting of Dox stress, our studies suggest ApoM can help sustain myocardial autophagic flux in a post-transcriptional manner, attenuate Dox cardiotoxicity, and prevent lysosomal injury. (J Am Coll Cardiol Basic Trans Science 2023;8:340–355) 

**ABBREVIATIONS AND ACRONYMS**

**AAV9** = adeno-associated virus 9
**Akt** = protein kinase B
**AMPK** = AMP-activated protein kinase
**ApoA-I** = apolipoprotein A-I
**ApoM** = apolipoprotein M
**Dox** = doxorubicin
**HDL** = high-density lipoprotein
**HF** = heart failure
**HW** = heart weight
**IP** = intraperitoneal
**LAMP1** = lysosomal associated membrane protein 1
**LV** = left ventricular
**LVEF** = left ventricular ejection fraction
**mTOR** = mammalian target of rapamycin
**RFP** = red fluorescent protein
**S1P** = sphingosine-1-phosphate
**S1PR3** = S1P receptor 3
**shRNA** = short hairpin RNA
**TFEB** = transcription factor EB
**TL** = tibia length
**TM** = triple mutant

Chemotherapeutic treatments improve survival for many patients with cancer, but these improvements are offset by increases in therapy-related cardiovascular mortality.[1] Anthracyclines, such as doxorubicin (Dox), are used for the treatment of cancers including breast cancer, leukemia, lymphoma, and sarcoma; however, the use of anthracyclines is limited by acute and chronic cardiotoxicity. The use of Dox remains common, particularly in children, with nearly 50% of children with cancer treated with an anthracycline.[2] In children with acute lymphoblastic leukemia treated with at least 1 dose of Dox, more than half have cardiovascular abnormalities in follow-up.[3] Although cardiotoxicity is clinically defined as a reduction in left ventricular (LV) ejection fraction (LVEF), reduced LV mass is also a clinical sign that portends a poor prognosis,[4] independent of changes in LVEF or body weight.[5] Long-term, anthracycline cardiotoxicity can result in heart failure (HF) in approximately 2% of patients, a diagnosis that carries a grave prognosis.[6-8] Proposed mechanisms of Dox cardiotoxicity include DNA damage downstream of topoisomerase 2b,[9] mitochondrial iron overload,[10] and lysosomal injury with decreased nuclear translocation of transcription factor EB (TFEB), a master regulator of autophagy and lysosomal biogenesis.[11,12]

High-density lipoprotein (HDL) has been suggested as a potential therapeutic for Dox cardiotoxicity and HF.[13,14] Cell culture studies indicate that HDL attenuates cell death caused by Dox via sphingosine-1-phosphate (S1P), a bioactive sphingolipid that binds G protein-coupled receptors on cardiomyocytes.[15] More than 70% of S1P binds directly to the lipocalin apolipoprotein M (ApoM) on HDL particles, and the remainder of S1P is associated with albumin.[16] ApoM is secreted primarily by hepatocytes, and it is associated with ~5% of HDL particles (and <2% of low-density lipoprotein particles).[17-19]

ApoM exerts pleiotropic effects, including antioxidant and antiatherogenic actions,[20,21] regulation of inflammation,[21] endothelial protection,[16,22] and increased cell survival.[23] Hepatocyte-specific overexpression of human *APOM* in mice ($Apom^{TG}$) results in significant increases in plasma ApoM and S1P,[19] and ApoM-knockout mice ($Apom^{KO}$) exhibit 50% reductions in plasma S1P, with normal amounts of S1P on albumin.[16]

Our prior clinical observations demonstrate that reduced circulating ApoM is associated with increased mortality in HF patients.[24] In addition, we recently observed that reduced ApoM is closely linked to the adverse effects of diabetes on human HF with preserved ejection fraction.[25,26] In HF patients, ApoM is inversely associated with mortality

From the [a]Washington University School of Medicine, St Louis, Missouri, USA; [b]Perelman School of Medicine, University of Pennsylvania School of Medicine/Hospital of the University of Pennsylvania, Philadelphia, Pennsylvania, USA; [c]Hope Center, Washington University School of Medicine, St Louis, Missouri, USA; [d]John Cochran Veterans Affairs Medical Center, St Louis, Missouri, USA; [e]Beth Israel Deaconess, Harvard Medical School, Boston, Massachusetts, USA; [f]Virginia Commonwealth University, Richmond, Virginia, USA; [g]Hunter Holmes McGuire Veterans Affairs Medical Center, Richmond, Virginia, USA; [h]Wake Forest School of Medicine, Winston-Salem, North Carolina, USA; [i]Bristol Myers Squibb, Princeton, New Jersey, USA; [j]Indiana University, Indianapolis, Indiana, USA; [k]Department of Clinical Biochemistry, Rigshospitalet, University of Copenhagen, Copenhagen, Denmark; and the [l]Department of Biomedical Sciences, University of Copenhagen, Copenhagen, Denmark.

The authors attest they are in compliance with human studies committees and animal welfare regulations of the authors' institutions and Food and Drug Administration guidelines, including patient consent where appropriate. For more information, visit the Author Center.

Manuscript received March 9, 2022; revised manuscript received September 26, 2022, accepted September 26, 2022.

independent of HF subtype, ischemic heart disease, HDL cholesterol, or apolipoprotein A-I (ApoA-I), the main protein constituent of HDL.[24] Despite these observations, little is known about the in vivo mechanisms by which ApoM may improve HF survival. In the present study, we hypothesized that increasing ApoM would attenuate Dox cardiotoxicity. Using anthracycline cardiotoxicity murine models, we identify that ApoM is a novel regulator of the autophagy-lysosome pathway. These studies point toward a novel function of the ApoM/S1P axis in regulating the autophagy-lysosome pathway in the myocardium and may contribute to the observed associations between ApoM and HF survival.

## METHODS

**REAGENTS.** Doxorubicin hydrochloride (50 mg) was purchased from United States Pharmacopeia (R11760) and dissolved in 20 mL of molecular-grade water to get a 2.5-mg/mL stock, which was used in animal and cell experiments.

**RODENT STUDIES.** All murine studies were approved by the Institutional Animal Care and Use Committee at Washington University in St Louis or by the Danish Animal Experiments Inspectorate and were performed following the *Guide for the Care and Use of Laboratory Animals*.[27] Mice were maintained on a 12:12-hour light-dark schedule in a temperature-controlled specific pathogen-free facility and fed standard laboratory mouse chow. $Apom^{TG}$ and $Apom^{KO}$ mice were previously described.[16,19] *Myh6-Cre* mice were purchased from The Jackson Laboratory,[28] and $S1pr3^{KO}$ mice were previously described.[29] Detailed methods for the generation of Rosa-lysosomal associated membrane protein 1 (LAMP1)-red fluorescent protein (RFP) mice and ApoM-knockin control or triple mutant (TM) mice (ApoM-CTR or ApoM-TM, respectively) are provided in the supplement. In age- and sex-matched adult mice, cardiotoxicity was induced by intraperitoneal (IP) or intravenous (IV) injection of Dox at specified doses. Acute models used 1 dose of 20 mg/kg Dox, and chronic models used 5 mg/kg once weekly × 4 weeks, as previously described.[11,12,30] Single-dose IP injections were also performed with 10 mg/kg and conducted in 2 independent laboratories at Washington University in St Louis (St. Louis, Missouri, USA), and Copenhagen University (Copenhagen, Denmark). Echocardiography was performed as previously described[31] and read blindly by a cardiologist. LV mass and LVEF were obtained using the Vevostrain package in Vevo (Fujifilm Visualsonics). Leukemic mice were generated by intravenous injection of male mice with $5 \times 10^5$ acute promyelocytic leukemia cells.[32] After allowing 4 days for engraftment, animals were treated with Dox on days 4, 6, 8, 11, 13, and 15 at 4 mg/kg subcutaneously. On day 17, peripheral blood was obtained via the retro-orbital plexus under anesthesia, and white blood cell counts were obtained using an automated cell counter (Hemavet 950, Drew Scientific). The percentage of circulating acute promyelocytic leukemia cells in blood was determined by flow cytometry.

**HISTOLOGIC ANALYSES.** Histologic analyses were performed as previously described.[31,33] Electron microscopy was performed as previously described.[34]

**CYTOPLASM AND NUCLEAR PROTEIN EXTRACTION.** Cardiac tissues were fractionated into nucleus-enriched and cytoplasmic samples by using a CelLytic NuCLEAR Extraction kit (Sigma, Nxtract), as previously described.[35]

**INSOLUBLE PROTEIN ISOLATION.** Insoluble protein isolation was performed as previously described.[31]

**QUANTITATIVE REAL-TIME POLYMERASE CHAIN REACTION ANALYSIS.** Quantitative real-time polymerase chain reaction was performed as described.[31]

**WESTERN BLOT ANALYSIS.** Western blot was performed on mice tissue or human samples as previously described.[36,37]

**HUMAN SAMPLES AND ApoM DETERMINATION.** Circulating ApoM protein determination was performed from 2 independent cohorts. First, patients >18 years of age diagnosed with HER2-positive breast cancer and scheduled to receive adjuvant therapy (anthracyclines, taxanes, and trastuzumab) were recruited prospectively and consecutively from Massachusetts General Hospital, MD Anderson Cancer Center, and McGill University.[38,39] The study was approved by the Institutional Review Boards of the participating institutions, and all subjects provided informed consent. The typical cancer treatment regimen consisted of Dox 60 mg/m$^2$ and cyclophosphamide 600 mg/m$^2$ every 3 weeks for 4 cycles. At 3 months, all patients received paclitaxel 80 mg/m$^2$ and trastuzumab 2 mg/kg weekly for 12 weeks, followed by trastuzumab 6 mg/kg every 3 weeks for 1 year. ApoM was measured in plasma samples using the SomaScan aptamer-based proteomics platform, as previously described and validated.[24,40,41] Second, to determine the relationship between ApoM protein levels and mortality in anthracycline cardiotoxicity,

we included patients from PHFS (Penn Heart Failure Study) who had a history of anthracycline-induced cardiomyopathy. ApoM determination in this cohort was previously described.[24]

For assessment of insoluble p62 in the human myocardium, deidentified human heart tissue samples were obtained from the Human Heart Tissue Bank at the University of Pennsylvania as previously described.[42] Transmural LV samples from nonfailing donors (obtained from brain-dead donors with no clinical history of HF) or anthracycline-induced cardiomyopathy (obtained at the time of orthotopic heart transplantation) were obtained from the LV free wall, with epicardial fat excluded, and flash frozen in liquid nitrogen.

**STATISTICAL ANALYSES.** Data are presented as the mean ± SEM or median with 25th and 75th percentiles (IQR). Data were tested for assumptions of normality with the Shapiro-Wilk test. If the samples were normally distributed, a parametric statistical analysis was performed using the 2-tailed Student's *t*-test for 2-group comparisons, and comparisons among multiple groups were analyzed by analysis of variance with Dunn's or Sidak's post hoc testing for multiple pairwise comparisons. If the samples were not normally distributed, we performed Kruskal-Wallis testing for multiple group analysis with Dunn's post hoc testing or Mann-Whitney testing for 2 groups, or we performed log transformation of the data where noted. For categorical variables, we used the chi-square test or Fisher exact test, as appropriate. A mixed-effects model or repeated measures was used for changes in ApoM levels over time. For Kaplan-Meier analysis of survival curves, the log-rank test was used. Univariable Cox proportional hazards models were used to assess the relationship between ApoM and survival in the PHFS patients. Standardized HR values, defined as HR per 1 unit increase in the *z*-score, are presented along with 95% CIs. A *P* value of $<0.05$ was considered statistically significant, and all probability values presented are 2 tailed. Analyses were performed using the MATLAB statistics and machine learning toolbox (Matlab 2016b, MathWorks) or GraphPad Prism 9.0.0.

**STUDY APPROVAL.** All animal studies were approved by the Animal Studies Committee at Washington University School of Medicine or by the Danish Animal Experiments Inspectorate. Human studies were deemed exempt by the Washington University School of Medicine Institutional Review Board because only deidentified human samples were used.

Additional methodology is described in the Supplemental Appendix.

## RESULTS

**ApoM IS INVERSELY ASSOCIATED WITH MORTALITY IN ANTHRACYCLINE CARDIOMYOPATHY.** We previously reported that circulating ApoM is inversely associated with mortality in HF patients.[24] Whether ApoM is associated with mortality in patients with anthracycline cardiomyopathy is presently unknown. To test this, we identified patients in the PHFS with a history of anthracycline cardiomyopathy (n = 46). Patient characteristics are shown in Supplemental Table 1. Among patients with a history of anthracycline cardiomyopathy, 11 patients died during follow-up. Baseline ApoM levels below the median were associated with reduced survival (**Figure 1A**). In univariable Cox proportional hazards models, we observed an inverse association between baseline ApoM and risk of death (**Figure 1B**) (standardized HR: 0.47; 95% CI: 0.25-0.88; $P = 0.018$).

Given the known cardiotoxicity caused by anthracyclines,[43] we tested whether anthracyclines reduce ApoM in humans and mice. We observed a decrease in circulating ApoM in breast cancer patients (clinical information shown in Supplemental Table 2) treated with anthracyclines for 4 cycles (**Figure 1C**). In murine studies, we observed parallel reductions in circulating ApoM after acute Dox administration (**Figures 1D and 1E**), an effect that was dose and time dependent (**Figures 1F and 1G**). Furthermore, mice with heterozygous ApoM deletion ($Apom^{+/-}$) exhibited increased mortality compared to littermate controls (**Figure 1H**), an effect that was independent of biological sex.

**ApoM ATTENUATES DOX-INDUCED CARDIOTOXICITY.** Given the reduction in plasma ApoM caused by Dox, we investigated whether increasing ApoM was sufficient to attenuate Dox cardiotoxicity. In initial studies comparing $Apom^{TG}$ to nontransgenic littermate controls, we modeled cardiotoxicity using high-dose, acute treatment with Dox (20 mg/kg IP). In these experiments, we observed that $Apom^{TG}$ mice were protected from Dox-induced reductions in murine ApoM, as well as the LV mass and heart weight (HW)/tibia length (TL) that occurred in littermate controls (**Figures 2A to 2D**). In chronic studies with Dox delivered via tail vein injection (5 mg/kg × 4 doses delivered once per week), we observed reductions in LVEF in littermate controls but not in $Apom^{TG}$ mice (**Figure 2E**). In chronic models, littermate control mice, but not $Apom^{TG}$ mice, demonstrated significantly reduced HW/TL (**Figure 2F**). To determine whether ApoM could be used therapeutically to attenuate Dox-induced

**FIGURE 1 ApoM Is Inversely Associated With Mortality in Anthracycline Cardiomyopathy**

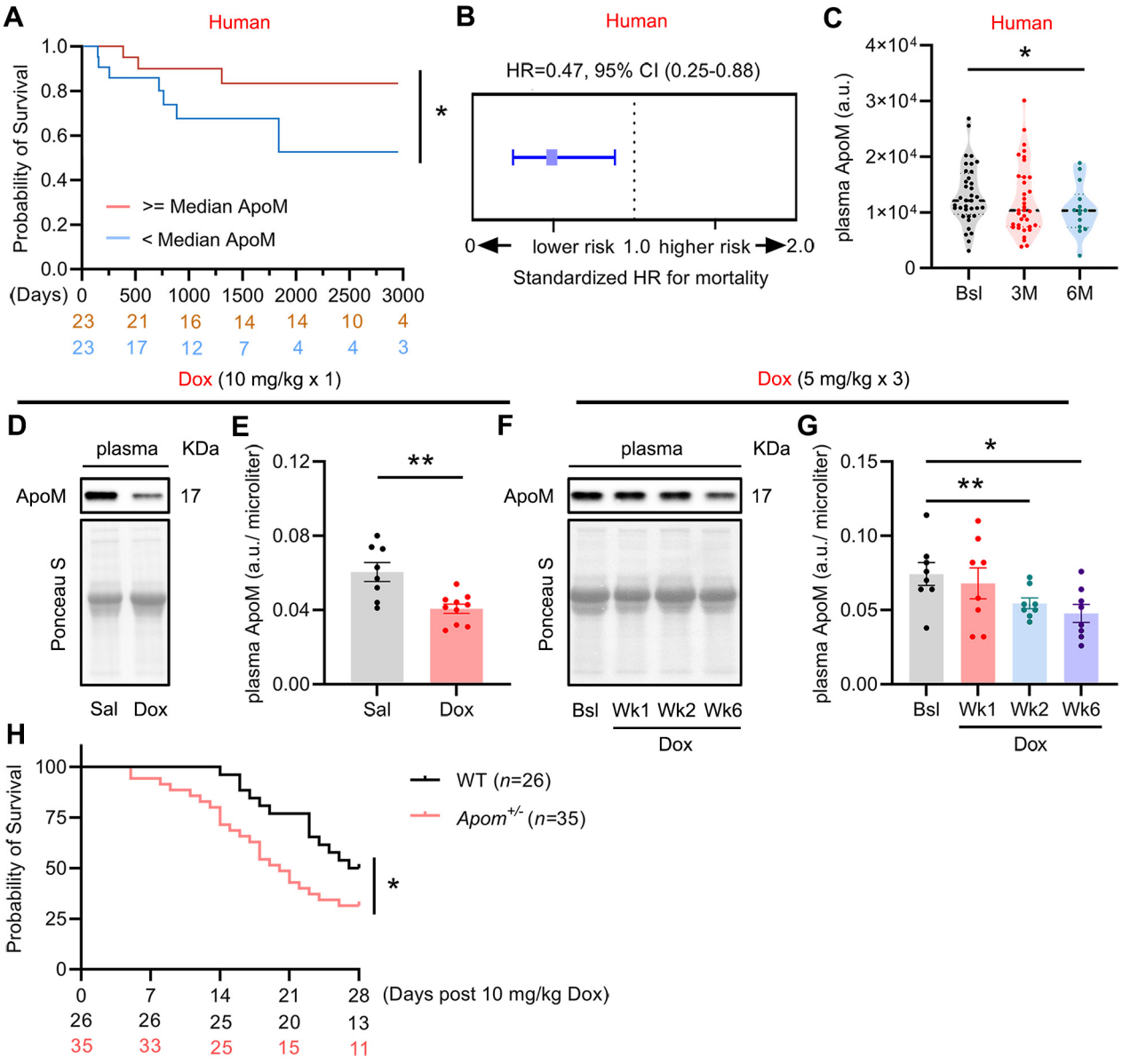


**(A)** Kaplan-Meier survival curves for all-cause mortality. The numbers of patients at risk at each timepoint are presented below the graph. **(B)** HR per SD ApoM in patients with anthracycline cardiomyopathy. Cox proportional hazards model, n = 46. **(C)** Aptamer-based ApoM plasma levels in patients with breast cancer after 4 cycles of anthracycline. Mixed-effects model with Dunn's correction for multiple comparisons (n = 36 at baseline, n = 35 at 3 months, and n = 14 at 6 months). Each dot represents 1 patient. Dotted lines represent median and quartiles. **(D)** Representative Western blot for ApoM from plasma isolated from mice 48 hours after treatment with saline or 10 mg/kg doxorubicin intraperitoneally. **(E)** Quantification of **D**. Student's *t*-test (n = 8 saline vs n = 10 Dox). Each dot represents 1 mouse. **(F)** Representative Western blot for ApoM from plasma isolated from mice after treatment with saline or 5 mg/kg Dox intraperitoneally. Week 1 means 48 hours after the first dose, week 2 means 48 hours after the second dose, and week 6 means 6 weeks after the first dose. **(G)** Quantification of **F**. One-way repeated-measures analysis of variance with Dunn's correction for multiple comparisons (n = 8 per group). Each dot represents 1 mouse. **(H)** Survival of littermate control (WT) and *Apom*$^{+/-}$ mice 4 weeks after 10 mg/kg Dox intraperitoneally (n = 26 WT vs n = 35 *Apom*$^{+/-}$ with sex matching). Log-rank test. *$P < 0.05$. **$P < 0.01$. 3M = 3 months; 6M = 6 months; ApoM = apolipoprotein M; a.u. = arbitrary units; Bsl = baseline; Dox = doxorubicin; Sal = saline; Wk = week; WT = wild type.

**FIGURE 2 ApoM Attenuates Dox-Induced Mortality and Cardiotoxicity**

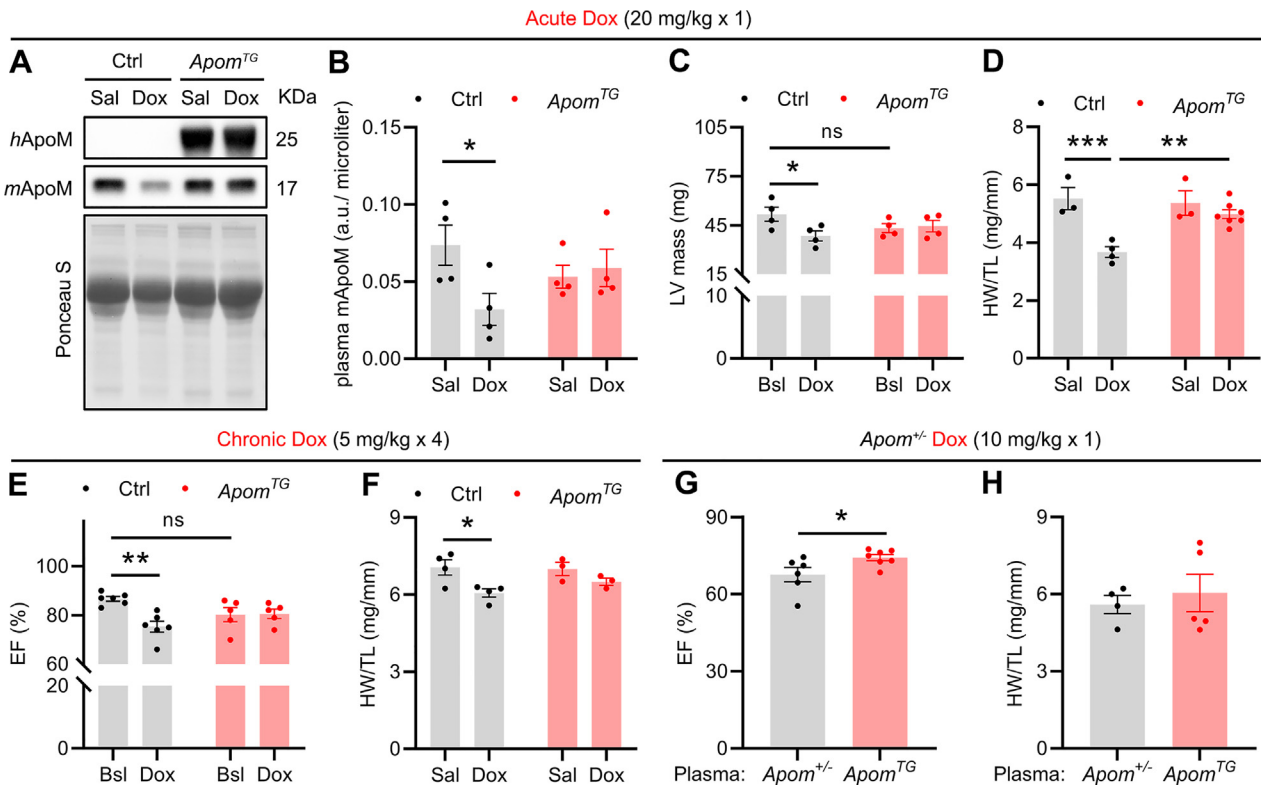


**(A)** Representative Western blot of human and mouse ApoM of plasma obtained from littermate control and *Apom*$^{TG}$ male mice 5 days after 20 mg/kg Dox intraperitoneally (IP). **(B)** Quantification of **A**. Two-way analysis of variance (ANOVA) with Sidak's correction for multiple comparisons (n = 4 per group). **(C)** Change in LV mass from baseline and 5 days after 20 mg/kg Dox intraperitoneally (IP). Two-way repeated-measures ANOVA with Sidak's correction for multiple comparisons (n = 4 per group male mice). **(D)** HW/TL from saline and 5 days after 20 mg/kg Dox IP. Two-way ANOVA with Sidak's correction for multiple comparisons (n = 3-7 male mice). **(E)** Change in LVEF from baseline and 3 months after 4 weekly doses of 5 mg/kg Dox intravenously (IV). Two-way repeated-measures ANOVA with Sidak's correction for multiple comparisons (n = 6 Ctrl vs n = 5 *Apom*$^{TG}$ male mice). **(F)** HW/TL from saline and 3 months after 4 weekly doses of 5 mg/kg Dox IV. Two-way ANOVA with Sidak's correction for multiple comparisons (n = 3-4 male mice). **(G)** Left ventricular ejection fraction in *Apom*$^{+/-}$ male mice treated with 120 μL plasma obtained from *Apom*$^{+/-}$ or *Apom*$^{TG}$ donor mice (2 doses on subsequent days) and 10 mg/kg Dox IP (on day 2). Student's *t*-test (n = 6 *Apom*$^{+/-}$ vs n = 7 *Apom*$^{TG}$ mice). **(H)** HW/TL in surviving mice from **G**, obtained at 4 weeks. Student's *t*-test (n = 4 *Apom*$^{+/-}$ vs n = 5 *Apom*$^{TG}$ mice). Each dot represents 1 mouse in **B to H**. **P* < 0.05. ***P* < 0.01. ****P* < 0.001. Ctrl = control; EF = ejection fraction; *h* = human; HW = heart weight; LV = left ventricular; *m* = mouse; ns = not significant; TL = tibia length; other abbreviations as in Figure 1.

cardiotoxicity, we treated *Apom*$^{+/-}$ mice with either ApoM transgenic or control (ApoM heterozygous) plasma before Dox followed by echocardiography at 14 days, before the onset of significant mortality (see Figure 1H). Of the 7 *Apom*$^{+/-}$ mice that received control plasma, 1 died before echocardiography, but 2 additional died before being sacrificed, whereas among the 7 mice that received transgenic plasma, all mice survived 14 days, and 2 mice died before being sacrificed. Mice that received plasma enriched for ApoM had higher LVEF than mice that received control plasma (Figure 2G), and HW/TL ratios were similar (Figure 2H).

Finally, using a murine model of acute promyelocytic leukemia,[32,44] we observed that Dox treatment (subcutaneous 4 mg/kg × 6 doses) (Supplemental Figure 1A) extended survival to a similar degree in *Apom*$^{TG}$ mice compared to littermate controls (Supplemental Figure 1B) with blast suppression 2 days after the last dose of Dox (Supplemental Figure 1C), indicating that ApoM does not attenuate the antileukemic efficacy of Dox in vivo.

**ApoM OVEREXPRESSION DOES NOT ALTER DOX-INDUCED DNA DAMAGE, APOPTOSIS, FIBROSIS, OR PROTEIN KINASE B SIGNALING.** We next investigated mechanisms by which ApoM could attenuate Dox cardiotoxicity. In these studies, we used an intermediate dose of Dox (10 mg/kg [IP]) sufficient to result in signaling changes without significant weight loss over 48 hours. We examined myocardial γ-H2AX foci[45] as a marker of DNA damage resulting from acute Dox administration, and found no difference in foci in $Apom^{TG}$ vs littermate control mice (Supplemental Figure 2). Because HDL can attenuate apoptosis caused by Dox in vitro,[15] we performed anti-caspase 3 immunohistochemistry in myocardial sections from the described mice and again found no significant differences in active nuclear caspase 3[46] (Supplemental Figure 3). Furthermore, the levels of myocardial anti-caspase 3 staining were relatively modest compared to positive controls obtained from prior closed-chest ischemia reperfusion experiments.[47] Evaluation of mitochondrial ultrastructure by electron microscopy did not demonstrate marked differences in acute or chronic Dox cardiotoxicity models between $Apom^{TG}$ and littermate controls (Supplemental Figures 4A and 4B), nor was there evidence of reduced fibrosis by Masson's trichrome stain in the chronic model (Supplemental Figure 5).

Transgenic overexpression of ApoA-I ($Apoa1^{TG}$), the main protein constituent of HDL, attenuates Dox cardiotoxicity via the phosphoinositol-3-kinase/protein kinase B (Akt) pathway.[14] We confirmed that $Apoa1^{TG}$ mice exhibited increased Akt phosphorylation at Ser473; however, we did not observe increased phosphorylation of Akt at Ser473 in $Apom^{TG}$ mice (Supplemental Figures 6A to 6D). Altogether, these studies suggest that ApoM did not attenuate cardiotoxicity in Dox cardiotoxicity by affecting DNA damage, apoptosis, Akt signaling, or fibrosis in the myocardium.

**ApoM OVEREXPRESSION PREVENTS DOX-INDUCED AUTOPHAGIC IMPAIRMENT.** We therefore turned our attention to whether ApoM might be affecting autophagy and lysosome dysfunction, which have recently been reported in murine models of Dox cardiotoxicity.[11,12] To measure autophagic flux, we performed immunohistochemistry for autophagy proteins LC3, a marker of autophagosomes, and p62, an autophagy receptor and substrate, respectively, from myocardial sections of mice treated with vehicle and Dox plus or minus the lysosomal inhibitor chloroquine. Compared to littermate controls, $Apom^{TG}$ exhibited intact autophagic flux after Dox, as evidenced by accumulation of LC3 (**Figures 3A and 3B**) and p62 (**Figures 3C and 3D**) with chloroquine. Importantly, $Apom^{TG}$ did not affect messenger RNA abundance of LC3B or p62 (**Figures 3E and 3F**), nor did $Apom^{TG}$ affect basal autophagic flux as determined by LC3 and p62 protein levels (Supplemental Figures 7A and 7B).

To verify the effect of ApoM on autophagy, we generated a new line of mice with human ApoM overexpression in the murine ApoM-knockout background ($Apom^{KO}Apom^{TG}$) and assayed accumulation of insoluble p62, an indicator of autophagic impairment that occurs in human and murine HF.[31,48] In contrast to Dox-treated $Apom^{KO}$ mice that accumulated insoluble p62, $Apom^{KO}Apom^{TG}$ mice exhibited reduced insoluble p62 (**Figures 3G and 3H**), which likely reflects increased autophagic removal of insoluble protein. We then confirmed that accumulation of insoluble p62 is a pathophysiologic feature of human anthracycline cardiomyopathy, because LV myocardium from anthracycline cardiomyopathy patients exhibited increased insoluble p62 relative to donors without a history of HF (**Figures 3I and 3J**).

**ApoM REGULATES TFEB IN AN S1P-DEPENDENT MANNER.** Prior studies suggest that increasing TFEB alleviates anthracycline cardiotoxicity.[12] To determine the effects of ApoM on nuclear translocation of TFEB, we performed nuclear protein isolation from control and $Apom^{TG}$ hearts. Although ApoM overexpression did not alter total TFEB protein levels (Supplemental Figures 8A and 8B), $Apom^{TG}$ mice demonstrated unexpected reductions in active nuclear TFEB at baseline (**Figures 4A and 4B**), as evidenced by reductions in the faster-migrating dephosphorylated band that represents active TFEB. Nevertheless, in response to Dox, $Apom^{TG}$ mice were resistant to the further decreases in nuclear TFEB that occurred in littermate controls (interaction $P < 0.001$) (**Figures 4C and 4D**), suggesting that in the context of ApoM overexpression, Dox has a differential effect on nuclear TFEB content.

To test whether an acute increase in ApoM also alters nuclear TFEB content, we used plasma transfer from donor $Apom^{TG}$ or $Apom^{KO}$ mice to recipient $Apom^{KO}$ mice before the administration of Dox. Plasma transfer increased human ApoM levels in $Apom^{KO}$ mice (Supplemental Figure 8C). $Apom^{TG}$ plasma also reduced baseline TFEB levels (that were elevated in $Apom^{KO}$ mice receiving $Apom^{KO}$ plasma) and attenuated further decrease in TFEB levels after Dox (interaction $P = 0.006$) (**Figures 4E and 4F**), similar to what we observed in $Apom^{TG}$ mice. Mechanistically, administration of $Apom^{TG}$ plasma resulted in increased phosphorylation of mammalian target of

**FIGURE 3** **ApoM Attenuates Dox-Induced Autophagic Impairment**

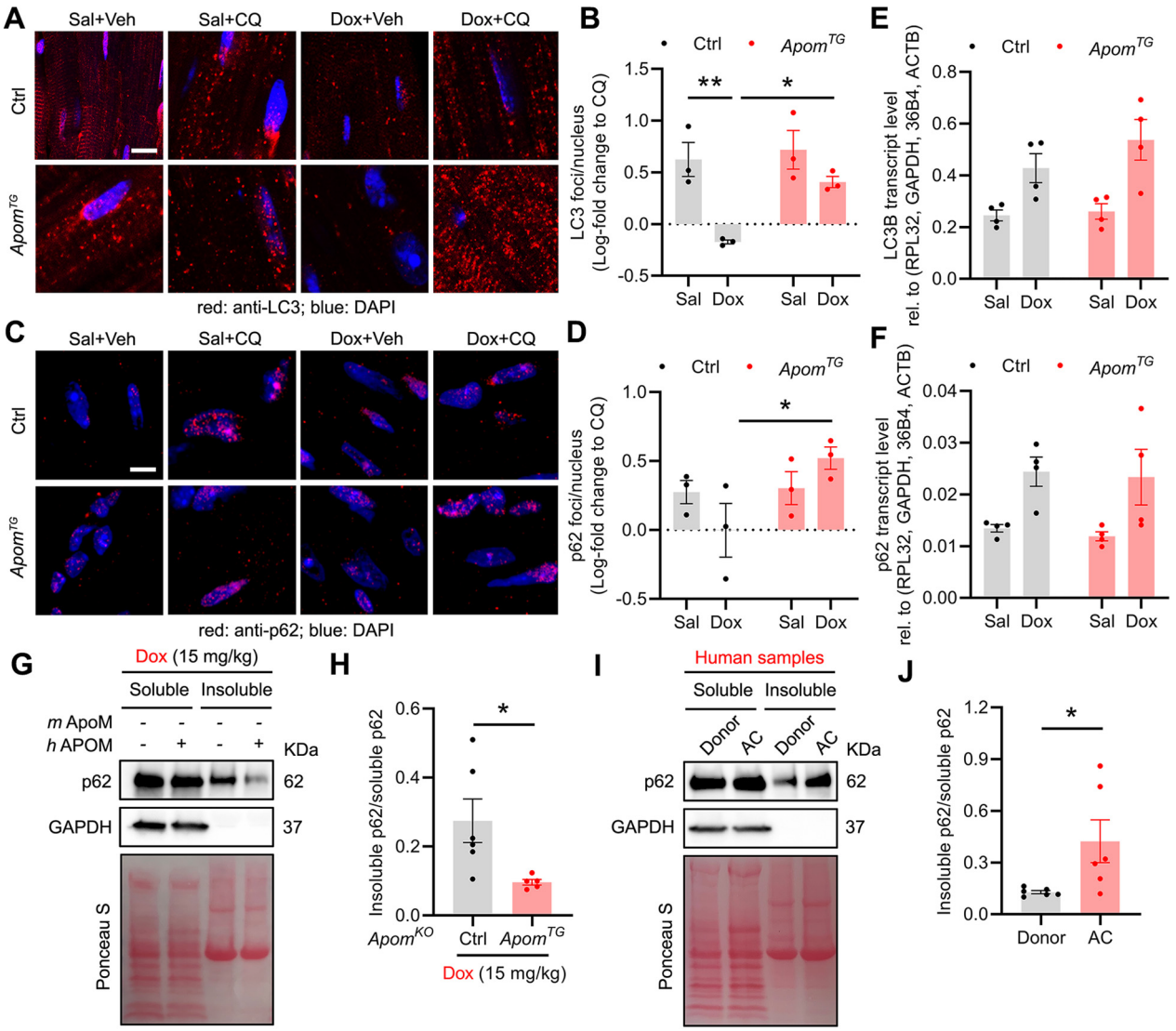


**(A)** Representative images of immunohistochemical staining of midmyocardial sections with α-LC3 and DAPI in littermate control (Ctrl) and *Apom*$^{TG}$ male mice 48 hours posttreatment with saline or Dox (10 mg/kg) intraperitoneally (IP) and, 4 hours before being sacrificed, with vehicle vs chloroquine (60 mg/kg) IP (scale bar = 5 μm). **(B)** Blinded quantification of LC3 foci from **A**. Two-way analysis of variance (ANOVA) with Sidak's correction for multiple comparisons (n = 3 per group). Data were log transformed because of violation of normality. **(C)** Representative images of immunohistochemical staining of midmyocardial sections with α-p62 and DAPI in mice from **A** (scale bar = 5 μm). **(D)** Blinded quantification of p62 foci from **C**. Two-way ANOVA with Sidak's correction for multiple comparisons (n = 3 per group). Data were log transformed because of violation of normality. **(E, F)** LC3B and p62 messenger RNA abundance accessed by quantitative polymerase chain reaction in Ctrl and *Apom*$^{TG}$ male mice 48 hours posttreatment with saline or 10 mg/kg Dox IP. Two-way ANOVA with Sidak's correction for multiple comparisons (n = 4 per group). **(G)** Representative Western blot for myocardial soluble vs insoluble p62 from *Apom*$^{KO}$ and *Apom*$^{KO}$*Apom*$^{TG}$ male mice 5 days after 15 mg/kg Dox IP. **(H)** The ratio of insoluble p62/total protein (based on Ponceau S) relative to the soluble p62/total protein. Student's *t*-test (n = 6 *Apom*$^{KO}$ vs n = 5 *Apom*$^{KO}$*Apom*$^{TG}$). **(I)** Representative Western blot for myocardial soluble vs insoluble p62 from patients with a history of heart failure caused by anthracycline cardiomyopathy vs donor controls obtained from patients without any known clinical heart failure. **(J)** The ratio of insoluble p62/total protein relative to the soluble p62/total protein. Student's *t*-test (n = 6 per group). Each **dot** represents 1 mouse in **B**, **D**, **E**, **F**, **and H** or 1 patient in **J**. *$P < 0.05$. **$P < 0.01$. AC = anthracycline cardiomyopathy; CQ = chloroquine; DAPI = 4′,6-diamidino-2-phenylindole; rel. = relative; Veh = vehicle; other abbreviations as in Figures 1 and 2.

**FIGURE 4 ApoM Attenuates Dox-Induced Reductions in Nuclear TFEB**

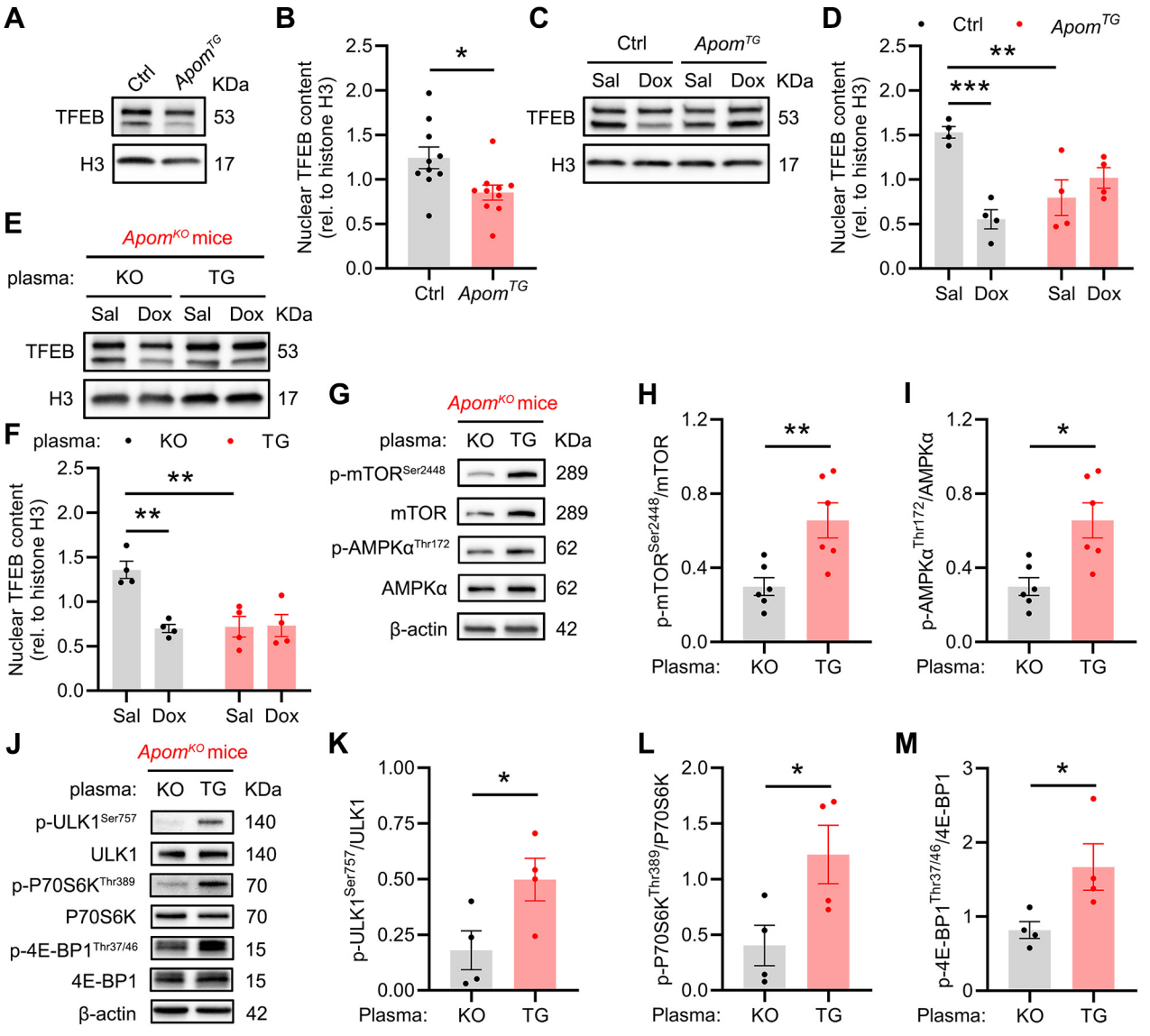


**(A)** Representative Western blot of TFEB from isolated myocardial nuclear protein extracts from littermate control (Ctrl) and *Apom*$^{TG}$ male mice. **(B)** Quantification of nuclear TFEB from **A**. Student's *t*-test (n = 10 per group). **(C)** Representative Western blot of TFEB from isolated myocardial nuclear protein extracts from Ctrl and *Apom*$^{TG}$ male mice 48 hours after treatment with saline or Dox (10 mg/kg) IP. **(D)** Quantification of nuclear TFEB from **C**. Two-way analysis of variance (ANOVA) with Sidak's correction for multiple comparisons (n = 4 per group). **(E)** Representative Western blot of TFEB from isolated myocardial nuclear protein extracts of *Apom*$^{KO}$ male mice 2 days after transfer of 120 μL plasma obtained from *Apom*$^{KO}$ or *Apom*$^{TG}$ donor mice 48 hours after treatment with saline or Dox (10 mg/kg) intraperitoneally. **(F)** Quantification of nuclear TFEB from **E**. Two-way ANOVA with Sidak's correction for multiple comparisons (n = 4 per group). **(G)** Representative Western blot of p-mTOR (Ser244), mTOR, p-AMPKα (Thr172), and AMPKα from myocardial protein extracts obtained from *Apom*$^{KO}$ male mice 2 days after transfer of 120 μL plasma obtained from *Apom*$^{KO}$ (KO) or *Apom*$^{TG}$ (TG) donor mice. **(H, I)** Quantification of p-mTOR$^{Ser2448}$/mTOR and p-AMPKα$^{Thr172}$/AMPKα from **G**. Student's *t*-test (n = 6 per group). **(J)** Representative Western blot of p-ULK1 (Ser757), ULK1, p-P70S6K (Thr389), P70S6K, p-4E-BP1 (Thr37/46), and 4E-BP1 from myocardial protein extracts obtained from *Apom*$^{KO}$ male mice 2 days after transfer of 120 μL plasma obtained from *Apom*$^{KO}$ (KO) or *Apom*$^{TG}$ (TG) donor mice. **(K to M)** Quantification of p-ULK1$^{Ser757}$/ULK1, p-P70S6K$^{Thr389}$/P70S6K, and p-4E-BP1$^{Thr37/46}$/4E-BP1 from **J**. Student's *t*-test (n = 4 per group). Each dot represents 1 mouse in **B**, **D**, **F**, **H**, **I**, and **K to M**. **P* < 0.05. ***P* < 0.01. ****P* < 0.001. AMPK = AMP-activated protein kinase; H3 = histone H3; mTOR = mammalian target of rapamycin; p- = phosphorylated; TFEB = transcription factor EB; other abbreviations as in Figures 1 to 3.

**FIGURE 5** ApoM Reduces Nuclear TFEB in an S1P-Dependent Manner Through S1PR3

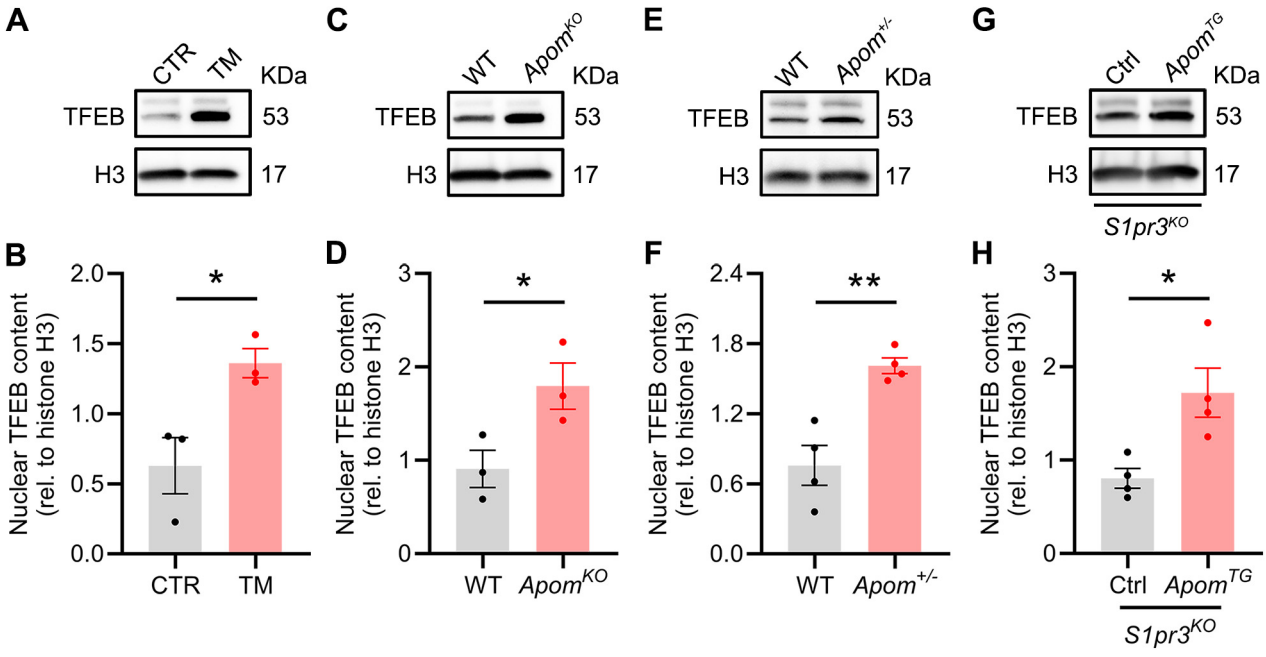


**(A)** Representative Western blot of TFEB from isolated myocardial nuclear protein extracts from control (CTR) and ApoM triple mutant (TM) male mice that cannot bind S1P. **(B)** Quantification of nuclear TFEB from **A**. Student's *t*-test (n = 3 per group). **(C)** Representative Western blot of TFEB from isolated myocardial nuclear protein extracts from WT and $Apom^{KO}$ male mice. **(D)** Quantification of nuclear TFEB from **C**. Student's *t*-test (n = 3 per group). **(E)** Representative Western blot of TFEB from isolated myocardial nuclear protein extracts from WT and $Apom^{+/-}$ male mice. **(F)** Quantification of nuclear TFEB from **E**. Student's *t*-test (n = 4 per group). **(G)** Representative Western blot of TFEB from isolated myocardial nuclear protein extracts in $Apom^{TG}$ mice crossed with $S1pr3^{KO}$ mice. **(H)** Quantification of nuclear TFEB from **G**. Student's *t*-test (n = 4 per group male mice). Each **dot** represents 1 mouse in **B, D, F, and H**. $^{*}P < 0.05$. $^{**}P < 0.01$. S1P = sphingosine-1-phosphate; S1PR3 = sphingosine-1-phosphate receptor 3; other abbreviations as in Figures 1, 3, and 4.

rapamycin (mTOR) at Ser2448 but also increased adenosine monophosphate-activated protein kinase (AMPK) phosphorylation at Thr172 and phosphorylation of multiple mTOR targets including ULK1, p70S6K, and 4E-BP1 (Figures 4G to 4M).

We next sought to determine whether our observation regarding TFEB regulation by ApoM requires canonical S1P-dependent signaling. To do so, we used a novel ApoM knockin mouse (R98A, W100A, and R116A) called ApoM-TM that cannot bind S1P. ApoM-TM mice demonstrated increased nuclear TFEB (Figures 5A and 5B), which phenocopied $Apom^{KO}$ and $Apom^{+/-}$ mice (Figures 5C to 5F). Finally, knockout of S1P receptor 3 (S1PR3) also abrogated the effects of ApoM on TFEB (Figures 5E and 5F), suggesting that ApoM negatively regulates TFEB through S1P-mediated S1PR3 signaling.

Given that ApoM overexpression reduced TFEB without reducing autophagic flux, we sought to explore the consequences of TFEB knockdown in littermate control and $Apom^{TG}$ mice, using a validated strategy of adeno-associated virus 9 (AAV9) short hairpin RNA (shRNA).[31] Littermate control and $Apom^{TG}$ mice were injected intravenously with 3.5e11 viral particles of AAV9-shScramble vs AAV9-shTFEB. AAV9-shTFEB transduction resulted in significant reductions in TFEB messenger RNA abundance in littermate controls and $Apom^{TG}$ mice (Figure 6A). TFEB knockdown had opposing effects on heart rate in littermate control vs $Apom^{TG}$ mice (interaction $P = 0.035$) (Figure 6B). Although TFEB knockdown did not significantly affect the EF (Figure 6C), $Apom^{TG}$ had significant increases in end-diastolic volume that did not occur in littermate controls (interaction $P = 0.045$) (Figure 6D); hence, in contrast to littermate controls, $Apom^{TG}$ mice had adverse LV remodeling after TFEB knockdown. To determine the effect of TFEB knockdown on autophagy, we performed immunostaining for LC3 in littermate control and $Apom^{TG}$ mice transduced with AAV9-shScramble or shTFEB. In comparison to mice transduced with shScramble, only $Apom^{TG}$ transduced with

**FIGURE 6 ApoM, TFEB, and Anthracycline Cardiotoxicity**

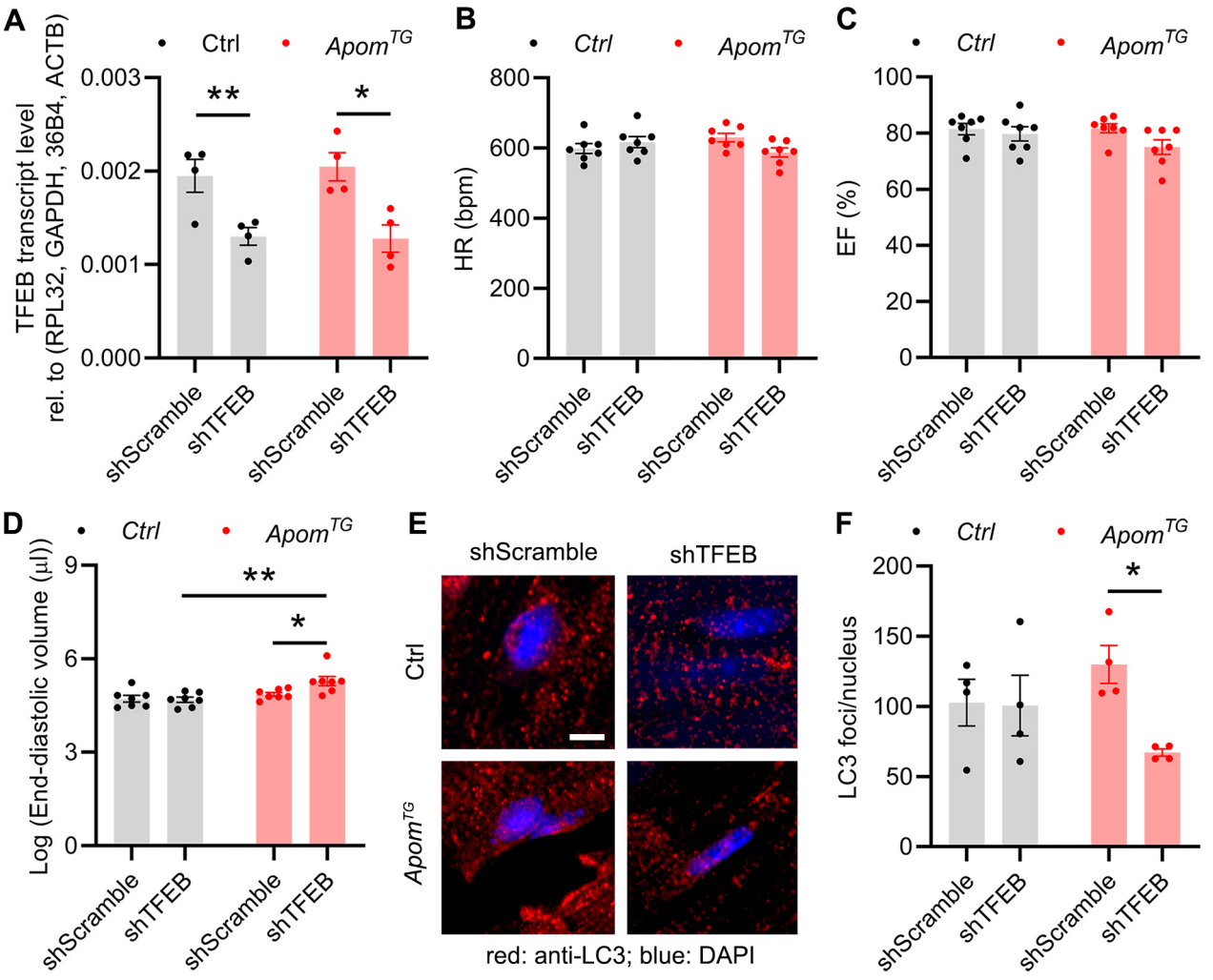


**(A)** TFEB messenger RNA abundance accessed by quantitative polymerase chain reaction in littermate control (Ctrl) and *Apom*$^{TG}$ male mice transduced with AAV9-shScramble or AAV9-shTFEB. Two-way analysis of variance (ANOVA) with Sidak's correction for multiple comparisons (n = 4 per group). **(B-D)** Heart rate, EF, and log-transformed end-diastolic volume assessed by echocardiography 2 weeks after viral transduction. Two-way ANOVA with Sidak's correction for multiple comparisons (n=7 per group). **(E)** Representative images of immunohistochemical assessment of LC3 foci in myocardial sections (scare bar = 5 μm). **(F)** Blinded quantification of LC3 foci from **E**. Two-way ANOVA with Sidak's correction for multiple comparisons (n = 4 per group). Each **dot** represents 1 mouse in **A to D and F**. *$P$ < 0.05. **$P$ < 0.01. AAV9 = adeno-associated virus 9; DAPI = 4′,6-diamidino-2-phenylindole; sh = short hairpin; other abbreviations as in Figures 2 and 4.

AAV9-shTFEB exhibited reductions in LC3 foci (Figures 6E and 6F). In littermate control wild-type mice, TFEB knockdown had no effect on LC3 foci, whereas TFEB knockdown in *Apom*$^{TG}$ mice reduced LC3 foci. In summary, *Apom*$^{TG}$ mice exhibit decreased nuclear TFEB and are sensitive to further knockdown of TFEB.

**ApoM AND S1P ATTENUATE DOX-INDUCED LYSOSOMAL INJURY.** Both anthracyclines and other chemotherapeutic drugs activate a lysosomal stress response characterized by loss of lysosomal pH[11] and lysosomal exocytosis, as evidenced by redistribution of lysosomes to the plasma membrane.[49] Given the paradoxical findings that ApoM preserves autophagic flux after Dox but reduces baseline nuclear levels of TFEB, a transcription factor that regulates autophagy and lysosomal biogenesis, we reasoned that ApoM and S1P may protect against Dox-induced lysosomal injury in vivo. To test this, we used a lysosomal RFP reporter (*Myh6-Cre* LAMP1-RFP) to genetically label and track

**FIGURE 7** **ApoM and S1P Attenuate Dox-Induced Lysosomal Injury**

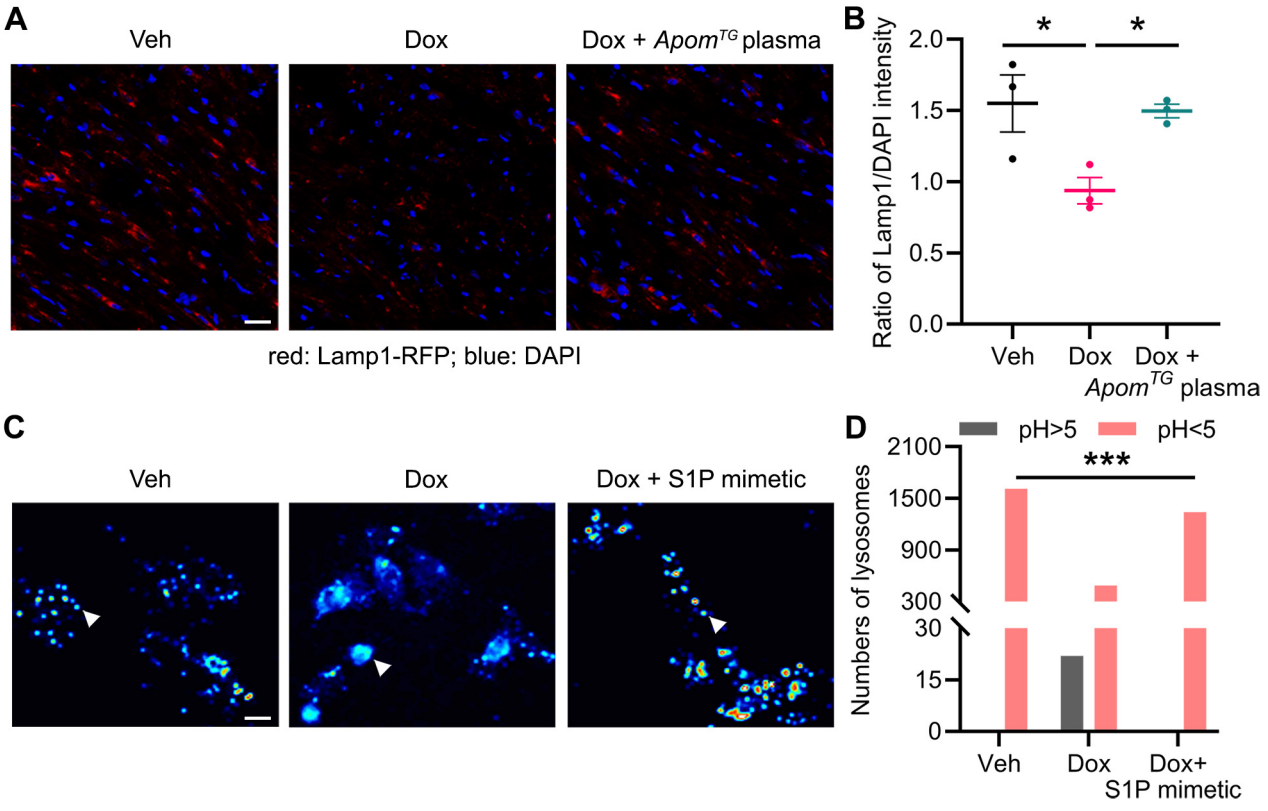


**(A)** Representative images of red fluorescence of midmyocardial sections in *Myh6-Cre* × Rosa-LAMP1-RFP mice injected with 120 μL plasma obtained from *Apom*$^{TG}$ mice and then treated with 2 days of Dox (10 mg/kg) intraperitoneally. **(B)** Blinded quantification of red/blue intensity from **A**. One-way analysis of variance with Sidak's correction for multiple comparisons (n = 3 per sex-matched group). Each **dot** represents 1 mouse. **(C)** S1P mimetic pretreatment of neonatal rat cardiomyocytes attenuates lysosomal injury. Representative pseudocolor excitation ratio images of Lysosensor-loaded lysosomes in cells exposed to DMSO, 0.5 μmol/L Dox, and 0.5 μmol/L Dox with 25 nmol/L FTY720 pretreatment for 5 minutes. Cells were incubated with 1 μmol/L Lysosensor Yellow/Blue DND 160 for 3 minutes, washed with Hank's balanced salt solution, and imaged by collecting pairs of images excited at 380 nm and 340 nm through a long-pass 480-nm emission filter through a 40×/1.35 oil immersion lens (Olympus). Frequency distribution of the excitation ratio values in single lysosomes (scale bar = 25 μm). **White arrows** indicate lysosomes. **(D)** Graph of the numbers of lysosomes with pH from **C**, and data for individual lysosomes pooled from 3 separate litters of rats were collected in 30 to 60 individual cells (chi-square test). *$P < 0.05$. ***$P < 0.001$. DMSO = dimethyl sulfoxide; LAMP1 = lysosomal associated membrane protein 1; RFP = red fluorescent protein; other abbreviations as in Figures 1, 3, and 5.

cardiomyocyte lysosomes (Supplemental Figure 9A). Expression of this LAMP1-RFP construct in cardiomyocytes does not significantly alter cardiac function or structure as measured by echocardiography (Supplemental Figures 9B and 9C) or significantly alter HW (Supplemental Figure 9D). We then treated *Myh6-Cre* Rosa-LAMP1-RFP mice with *Apom*$^{TG}$ plasma followed by Dox. Dox induced reductions in the RFP signal that were attenuated by *Apom*$^{TG}$ plasma (**Figures 7A and 7B**).

To further determine whether an S1P mimetic could attenuate lysosomal injury, we treated neonatal rat cardiomyocytes with either vehicle or the S1P mimetic FTY720 before treatment with Dox, followed by live cell microscopy with a Lysosensor DND-160, a pH-sensitive ratiometric probe that can be used to measure pH in acidified organelles. To harness only the S1P-activating effects of FTY720, cardiomyocytes were pretreated with 25 nmol/L of FTY720 for 5 minutes before washing the cells with phosphate-buffered saline and subsequent treatment with Dox. In these experiments, we were careful to treat with low-dose (0.5 μmol/L) Dox for only 4 hours to minimize the cytotoxic effects of the drug seen with higher doses and longer timepoints. Treatment of cardiomyocytes with Dox resulted in a characteristic pattern of lysosomal exocytosis that was abrogated by pretreatment with FTY720 (**Figures 7C and 7D**).

Furthermore, Dox resulted in acute changes in lysosomal pH over 4 hours that were attenuated by pretreatment with FTY720. Hence, both ApoM and a S1P mimetic are able to protect cardiomyocyte lysosomes from Dox-induced injury and alterations in pH, respectively.

## DISCUSSION

In this paper, we used a spectrum of human cohort and myocardial tissue samples as well as multiple murine models to demonstrate that ApoM attenuates the cardiotoxicity, autophagic impairment, and lysosomal injury that occurs because of anthracyclines. The translational relevance of our studies is highlighted by our observations that: 1) circulating ApoM is inversely associated with mortality in human anthracycline-induced cardiomyopathy; 2) anthracycline treatment reduces circulating ApoM in humans and mice; 3) increasing ApoM attenuates Dox cardiotoxicity and preserves myocardial autophagic flux but does not affect Dox antineoplastic efficacy; and 4) autophagic impairment is characteristic of human anthracycline cardiomyopathy. These findings are concordant with and expand on our prior findings that ApoM is inversely associated with all-cause mortality in HF patients.[24]

Mechanistically, our studies suggest ApoM, via S1P signaling, is a novel regulator of the autophagy-lysosome pathway and TFEB, both of which exhibit complex interactions in Dox cardiotoxicity. The main mechanistic conclusion of our work is that cardioprotection by ApoM and S1P[50,51] are mediated by effects of ApoM/S1P on lysosomes and preservation of autophagic flux. Although we find that ApoM administration leads to activation of mTOR signaling, which is typically associated with reduced autophagic flux, we find concomitant activation of AMPK. Simultaneous activation of mTOR and AMPK has previously been observed and may partially explain why ApoM does not reduce basal autophagy.[52]

Our findings further demonstrate that ApoM/S1P can protect lysosomes from Dox-induced loss of pH. Across all our models, we consistently observed that untreated wild-type mice have higher nuclear TFEB levels than $Apom^{TG}$ mice; hence, it is unlikely that the effect of ApoM/S1P on lysosomes is caused by increased TFEB nuclear translation. Although prior findings suggest that increased TFEB attenuates Dox cardiotoxicity, TFEB does not appear to play a role in $Apom^{+/-}$ mice because they exhibit increased nuclear TFEB and increased mortality after Dox. These findings suggest alternate potential mechanisms. In fact, our data indicate 2 distinct effects of ApoM/S1P on TFEB. In the unstressed heart before Dox exposure, ApoM/S1P signaling negatively regulates TFEB nuclear translocation. Mutation of the ApoM-S1P binding pocket, ApoM heterozygosity or knockout, and S1PR3 knockout all caused increases in myocardial nuclear TFEB content, suggesting that the ApoM/S1P axis is a rheostat for TFEB in the unstressed heart; that is, in the absence of exogenous stress, increasing ApoM reduces active TFEB content, whereas reducing ApoM or its ability to bind S1P or signal through S1PR3 all increase nuclear TFEB. Our data point toward mTOR phosphorylation as the most likely reason for TFEB down-regulation in $Apom^{TG}$ mice. Interestingly, mTOR inhibition was previously shown to exacerbate Dox cardiotoxicity by reducing LV mass, suggesting that ApoM-driven mTOR activation might partially explain the preserved LV mass observed in $Apom^{TG}$ mice treated with Dox. Given that mTOR inactivates TFEB and recent observations that increased TFEB may exacerbate HF outcomes,[53] it is possible that mTOR activation may prevent progression to cardiomyopathy through TFEB inhibition. Furthermore, in the setting of Dox, ApoM overexpression or delivery of plasma enriched for ApoM preserved both TFEB and lysosomal abundance in cardiomyocytes in vivo, as assayed by LAMP1-RFP–positive structures. The effect on cardiomyocyte lysosomes was also observed in vitro after a brief incubation with an S1P mimetic. This relatively rapid effect of ApoM/S1P is also consistent with a posttranscriptional mechanism, although one limitation of our current studies is that we have yet to identify how ApoM/S1P can protect lysosomal structures during Dox injury.

In our studies, we did not find significant effects of Dox or ApoM on cell death or fibrosis in models where mice received cumulative doses of Dox ranging from 10 to 20 mg/kg, well within the typical doses delivered in murine studies. However, the literature is mixed in terms of the degree of apoptosis and LV fibrosis attributable to Dox, with some reports describing 7.5% fibrotic area 4 days after Dox (10 mg/kg)[54] and other studies showed no increase in terminal deoxynucleotidyl transferase dUTP nick end labeling-positive cells and only perivascular fibrosis with a cumulative dose of 12 mg/kg.[55] In contrast, other studies of higher doses (20 mg/kg) show

minimal LV fibrosis after 2 weeks.[56] Although there is significant variability in the degree of LV fibrosis reported, one of the most consistent findings across murine and human studies is loss of LV mass, which is associated with increased morbidity and mortality in humans.[5,57,58] Whether acute therapy with ApoM or S1P mimetics, particularly for individuals with reduced ApoM, may attenuate reductions in LV mass requires further research.

Another important finding of our studies is that autophagic impairment is a pathophysiologic characteristic of anthracycline cardiomyopathy in humans. Although anthracyclines mediate toxicity via multiple pathways, lysosomes have recently emerged as a critical target of anthracyclines and other antineoplastic drugs,[11,12,49] and they have an increasingly recognized role in cardiometabolic disease.[59] In humans with anthracycline cardiomyopathy, we observed accumulation of insoluble p62, suggesting that the autophagic impairment observed previously in murine models[11] also occurs in humans. Our studies support that restoring ApoM might be an attractive cardioprotective strategy, because ApoM heterozygous loss of function increased Dox-associated mortality, whereas acute increases in ApoM demonstrated biological activity against Dox-induced lysosomal injury. In addition, because the preservation of autophagic flux has been implicated in the pathogenesis of HF more broadly,[31,48] our studies may help explain the broader link between ApoM and HF outcomes.

**STUDY LIMITATIONS.** Limitations of our study include that the observations regarding ApoM and outcomes of anthracycline cardiomyopathy are based on a small number of patents (n = 46) and events (n = 11). Although ApoM attenuates Dox-induced autophagic impairment, as determined by flux assays and accumulation of insoluble protein, the mechanisms for ApoM-mediated preservation of autophagic flux and lysosomal function remain incompletely defined and will require further experimental studies. Finally, the role of autophagy in Dox cardiomyopathy remains context dependent, and whether the salutary effects of ApoM relate to its effects on TFEB, autophagy, or lysosome function and how these pathways result in Dox cardiomyopathy will require additional studies.

## CONCLUSIONS

The major conclusions of our study are that anthracycline therapy reduces ApoM in humans and mice, and that reductions in ApoM are associated with mortality. Treatment of mice with ApoM attenuates anthracycline cardiotoxicity and markers of autophagic impairment. The most likely explanation for these findings is that ApoM attenuates anthracycline-induced lysosomal injury, thereby attenuating cardiotoxicity.

## FUNDING SUPPORT AND AUTHOR DISCLOSURES

Dr Javaheri was supported by R01HL155344 and K08HL138262 from the National Heart, Lung, and Blood Institute and by the Diabetes Research Center at Washington University in St Louis of the National Institutes of Health (NIH) under award number P30DK020579, as well as NIH grant P30DK056341 (Nutrition Obesity Research Center), and by the Children's Discovery Institute of Washington University (MC-FR-2020-919) and St Louis Children's Hospital. Dr Guo was supported by an American Heart Association Postdoctoral Fellowship (898679). Dr Diwan was supported by grants from the Department of Veterans Affairs (I01BX004235) and the NIH (HL107594, HL43431, and NS094692). Dr Scherrer-Crosbie is supported by R01HL130539 and R01HL131613. Dr Rawnsley was supported by training grant support from the NIH (T32007081). Dr Desai was supported by R01HL136603. Dr Bergom was supported by R01HL147884. Research reported in this publication was also supported by the National Cancer Institute of the NIH under award numbers R50CA211466 (Dr Rettig), R35CA210084 (Dr DiPersio), P01CA101937 (Dr DiPersio), and R01HL119962 (Dr Parks). Human heart tissue procurement was supported by the National Heart, Lung, and Blood Institute via R01HL105993 (Drs Margulies and Cappola). Drs Christoffersen and Hajny were supported by the Novo Nordisk Foundation (0053008 and NNF13OC0003898). Dr Stitziel was supported in part by R01HL131961, R01HL159171, P01HL151328, and UM1HG008853 and by the Foundation for Barnes-Jewish Hospital. We acknowledge support from the NIH Shared Instrumentation Grant (S10RR027552) for support through the Hope Center Neuroimaging Core, the Molecular Microbiology Imaging Facility, and the Advanced Imaging and Tissue Analysis Core of the Digestive Disease Research Core Center (DDRCC NIH P30DK052574) at Washington University School of Medicine. Dr Stitziel has received consulting fees from Sension Therapeutics and investigator-initiated research funding from Regeneron Pharmaceuticals unrelated to the content of this study. Dr Javaheri has a pending patent for fusion protein nanodiscs for the treatment of heart failure and eye diseases, receives research funding from AstraZeneca, and is on the Scientific Advisory Board of Mobius Scientific. All other authors have reported that they have no relationships relevant to the contents of this paper to disclose.

**ADDRESS FOR CORRESPONDENCE:** Dr Ali Javaheri, Washington University School of Medicine, CSRB 8818, St Louis, Missouri 63105, USA. E-mail: ali.javaheri@wustl.edu. Twitter: @Alicardsdoc.

## PERSPECTIVES

**COMPETENCY IN MEDICAL KNOWLEDGE:** ApoM is a lipocalin that is associated with high-density lipoprotein, and ApoM is inversely associated with mortality in human heart failure. Here, we have identified that anthracycline therapy is associated with reductions in ApoM in humans and that in patients with cardiomyopathy caused by anthracycline, ApoM is inversely associated with mortality. Patients with anthracycline-induced heart failure also exhibit impairments in autophagy, with accumulation of insoluble proteins, which is also evidenced in mice that lack ApoM.

**TRANSLATIONAL OUTLOOK:** By identifying ApoM as a mechanistic link between doxorubicin cardiotoxicity and autophagic impairment, our studies suggest that therapies that restore ApoM levels may prevent or treat anthracycline cardiomyopathy. Whether this mechanism is generalizable to other heart failure syndromes will require further study.

## REFERENCES

**1.** Sturgeon KM, Deng L, Bluethmann SM, et al. A population-based study of cardiovascular disease mortality risk in US cancer patients. *Eur Heart J*. 2019;40:3889–3897.

**2.** Armenian S, Bhatia S. Predicting and preventing anthracycline-related cardiotoxicity. *Am Soc Clin Oncol Educ Book*. 2018;38:3–12.

**3.** Lipshultz SE, Colan SD, Gelber RD, Perez-Atayde AR, Sallan SE, Sanders SP. Late cardiac effects of doxorubicin therapy for acute lymphoblastic leukemia in childhood. *N Engl J Med*. 1991;324:808–815.

**4.** Neilan TG, Coelho-Filho OR, Pena-Herrera D, et al. Left ventricular mass in patients with a cardiomyopathy after treatment with anthracyclines. *Am J Cardiol*. 2012;110:1679–1686.

**5.** Jordan JH, Castellino SM, Melendez GC, et al. Left ventricular mass change after anthracycline chemotherapy. *Circ Heart Fail*. 2018;11:e004560.

**6.** Nadruz W Jr, West E, Sengelov M, et al. Cardiovascular phenotype and prognosis of patients with heart failure induced by cancer therapy. *Heart*. 2019;105:34–41.

**7.** Hardaway BW. Adriamycin-associated cardiomyopathy: where are we now? Updates in pathophysiology, dose recommendations, prognosis, and outcomes. *Curr Opin Cardiol*. 2019;34:289–295.

**8.** Fornaro A, Olivotto I, Rigacci L, et al. Comparison of long-term outcome in anthracycline-related versus idiopathic dilated cardiomyopathy: a single centre experience. *Eur J Heart Fail*. 2018;20:898–906.

**9.** Zhang S, Liu X, Bawa-Khalfe T, et al. Identification of the molecular basis of doxorubicin-induced cardiotoxicity. *Nat Med*. 2012;18:1639–1642.

**10.** Ichikawa Y, Ghanefar M, Bayeva M, et al. Cardiotoxicity of doxorubicin is mediated through mitochondrial iron accumulation. *J Clin Invest*. 2014;124:617–630.

**11.** Li DL, Wang ZV, Ding G, et al. Doxorubicin blocks cardiomyocyte autophagic flux by inhibiting lysosome acidification. *Circulation*. 2016;133:1668–1687.

**12.** Bartlett JJ, Trivedi PC, Yeung P, Kienesberger PC, Pulinilkunnil T. Doxorubicin impairs cardiomyocyte viability by suppressing transcription factor EB expression and disrupting autophagy. *Biochem J*. 2016;473:3769–3789.

**13.** Diab A, Valenzuela Ripoll C, Guo Z, Javaheri A. HDL composition, heart failure, and its comorbidities. *Front Cardiovasc Med*. 2022;9:846990.

**14.** Durham KK, Kluck G, Mak KC, Deng YD, Trigatti BL. Treatment with apolipoprotein A1 protects mice against doxorubicin-induced cardiotoxicity in a scavenger receptor class B, type I-dependent manner. *Am J Physiol Heart Circ Physiol*. 2019;316:H1447–H1457.

**15.** Frias MA, Lang U, Gerber-Wicht C, James RW. Native and reconstituted HDL protect cardiomyocytes from doxorubicin-induced apoptosis. *Cardiovasc Res*. 2010;85:118–126.

**16.** Christoffersen C, Obinata H, Kumaraswamy SB, et al. Endothelium-protective sphingosine-1-phosphate provided by HDL-associated apolipoprotein M. *Proc Natl Acad Sci U S A*. 2011;108:9613–9618.

**17.** Christoffersen C, Nielsen LB, Axler O, Andersson A, Johnsen AH, Dahlback B. Isolation and characterization of human apolipoprotein M-containing lipoproteins. *J Lipid Res*. 2006;47:1833–1843.

**18.** Xu N, Dahlback B. A novel human apolipoprotein (apoM). *J Biol Chem*. 1999;274:31286–31290.

**19.** Liu M, Seo J, Allegood J, et al. Hepatic apolipoprotein M (apoM) overexpression stimulates formation of larger apoM/sphingosine 1-phosphate-enriched plasma high density lipoprotein. *J Biol Chem*. 2014;289:2801–2814.

**20.** Elsoe S, Ahnstrom J, Christoffersen C, et al. Apolipoprotein M binds oxidized phospholipids and increases the antioxidant effect of HDL. *Atherosclerosis*. 2012;221:91–97.

**21.** Christoffersen C, Jauhiainen M, Moser M, et al. Effect of apolipoprotein M on high density lipoprotein metabolism and atherosclerosis in low density lipoprotein receptor knock-out mice. *J Biol Chem*. 2008;283:1839–1847.

**22.** Christensen PM, Liu CH, Swendeman SL, et al. Impaired endothelial barrier function in apolipoprotein M-deficient mice is dependent on sphingosine-1-phosphate receptor 1. *FASEB J*. 2016;30:2351–2359.

**23.** Ruiz M, Okada H, Dahlback B. HDL-associated ApoM is anti-apoptotic by delivering sphingosine 1-phosphate to S1P1 & S1P3 receptors on vascular endothelium. *Lipids Health Dis*. 2017;16:36.

**24.** Chirinos JA, Zhao L, Jia Y, et al. Reduced apolipoprotein M and adverse outcomes across the spectrum of human heart failure. *Circulation*. 2020;141:1463–1476.

**25.** Hanff TC, Cohen JB, Zhao L, et al. Quantitative proteomic analysis of diabetes mellitus in heart failure with preserved ejection fraction. *J Am Coll Cardiol Basic Trans Science*. 2021;6:89–99.

**26.** Li H, Rosenzweig A. Understanding heart failure with preserved ejection fraction in a diabetic way. *J Am Coll Cardiol Basic Trans Science*. 2021;6:100–102.

**27.** National Research Council (US) Committee for the Update of the Guide for the Care and Use of Laboratory Animals. Guide for the Care and Use of Laboratory Animals. 8th ed. Washington (DC): National Academies Press (US); 2011.

**28.** Agah R, Frenkel PA, French BA, Michael LH, Overbeek PA, Schneider MD. Gene recombination in postmitotic cells. Targeted expression of Cre recombinase provokes cardiac-restricted, site-specific rearrangement in adult ventricular muscle in vivo. *J Clin Invest*. 1997;100:169–179.

**29.** Kono M, Mi Y, Liu Y, et al. The sphingosine-1-phosphate receptors S1P1, S1P2, and S1P3 function coordinately during embryonic angiogenesis. *J Biol Chem*. 2004;279:29367–29373.

**30.** Dhingra R, Rabinovich-Nikitin I, Rothman S, et al. Proteasomal degradation of TRAF2 mediates

mitochondrial dysfunction in doxorubicin-cardiomyopathy. *Circulation*. 2022;146:934–954.

**31.** Ma X, Mani K, Liu H, et al. Transcription factor EB activation rescues advanced αB-crystallin mutation-induced cardiomyopathy by normalizing desmin localization. *J Am Heart Assoc*. 2019;8:e010866.

**32.** Westervelt P, Lane AA, Pollock JL, et al. High-penetrance mouse model of acute promyelocytic leukemia with very low levels of PML-RARα expression. *Blood*. 2003;102:1857–1865.

**33.** Li Z, Guo Z, Lan R, et al. The poly(ADP-ribosyl)ation of BRD4 mediated by PARP1 promoted pathological cardiac hypertrophy. *Acta Pharm Sin B*. 2021;11:1286–1299.

**34.** Liu H, Javaheri A, Godar RJ, et al. Intermittent fasting preserves beta-cell mass in obesity-induced diabetes via the autophagy-lysosome pathway. *Autophagy*. 2017;13:1952–1968.

**35.** Ma X, Liu H, Murphy JT, et al. Regulation of the transcription factor EB-PGC1alpha axis by beclin-1 controls mitochondrial quality and cardiomyocyte death under stress. *Mol Cell Biol*. 2015;35:956–976.

**36.** Guo Z, Zhang Y, Liu C, Youn JY, Cai H. Toll-like receptor 2 (TLR2) knockout abrogates diabetic and obese phenotypes while restoring endothelial function via inhibition of NOX1. *Diabetes*. 2021;70:2107–2119.

**37.** Wang P, Lan R, Guo Z, et al. Histone demethylase JMJD3 mediated doxorubicin-induced cardiomyopathy by suppressing SESN2 expression. *Front Cell Dev Biol*. 2020;8:548605.

**38.** Sawaya H, Sebag IA, Plana JC, et al. Assessment of echocardiography and biomarkers for the extended prediction of cardiotoxicity in patients treated with anthracyclines, taxanes, and trastuzumab. *Circ Cardiovasc Imaging*. 2012;5:596–603.

**39.** Ky B, Putt M, Sawaya H, et al. Early increases in multiple biomarkers predict subsequent cardiotoxicity in patients with breast cancer treated with doxorubicin, taxanes, and trastuzumab. *J Am Coll Cardiol*. 2014;63:809–816.

**40.** Ngo D, Sinha S, Shen D, et al. Aptamer-based proteomic profiling reveals novel candidate biomarkers and pathways in cardiovascular disease. *Circulation*. 2016;134:270–285.

**41.** Mosley JD, Benson MD, Smith JG, et al. Probing the virtual proteome to identify novel disease biomarkers. *Circulation*. 2018;138:2469–2481.

**42.** Bedi KC Jr, Snyder NW, Brandimarto J, et al. Evidence for intramyocardial disruption of lipid metabolism and increased myocardial ketone utilization in advanced human heart failure. *Circulation*. 2016;133:706–716.

**43.** Cardinale D, Colombo A, Bacchiani G, et al. Early detection of anthracycline cardiotoxicity and improvement with heart failure therapy. *Circulation*. 2015;131:1981–1988.

**44.** Nervi B, Ramirez P, Rettig MP, et al. Chemosensitization of acute myeloid leukemia (AML) following mobilization by the CXCR4 antagonist AMD3100. *Blood*. 2009;113:6206–6214.

**45.** Kao J, Milano MT, Javaheri A, et al. Gamma-H2AX as a therapeutic target for improving the efficacy of radiation therapy. *Curr Cancer Drug Targets*. 2006;6:197–205.

**46.** Kamada S, Kikkawa U, Tsujimoto Y, Hunter T. Nuclear translocation of caspase-3 is dependent on its proteolytic activation and recognition of a substrate-like protein(s). *J Biol Chem*. 2005;280:857–860.

**47.** Javaheri A, Bajpai G, Picataggi A, et al. TFEB activation in macrophages attenuates post-myocardial infarction ventricular dysfunction independently of ATG5-mediated autophagy. *JCI Insight*. 2019;4:e127312.

**48.** Hartupee J, Szalai GD, Wang W, Ma X, Diwan A, Mann DL. Impaired protein quality control during left ventricular remodeling in mice with cardiac restricted overexpression of tumor necrosis factor. *Circ Heart Fail*. 2017;10:e004252.

**49.** Zhitomirsky B, Assaraf YG. Lysosomal accumulation of anticancer drugs triggers lysosomal exocytosis. *Oncotarget*. 2017;8:45117–45132.

**50.** Theilmeier G, Schmidt C, Herrmann J, et al. High-density lipoproteins and their constituent, sphingosine-1-phosphate, directly protect the heart against ischemia/reperfusion injury in vivo via the S1P3 lysophospholipid receptor. *Circulation*. 2006;114:1403–1409.

**51.** Swendeman SL, Xiong Y, Cantalupo A, et al. An engineered S1P chaperone attenuates hypertension and ischemic injury. *Sci Signal*. 2017;10:eaal2722.

**52.** Dalle Pezze P, Ruf S, Sonntag AG, et al. A systems study reveals concurrent activation of AMPK and mTOR by amino acids. *Nat Commun*. 2016;7:13254.

**53.** Evans S, Finck B, Weinheimer C, et al. Targeting the autophagy-lysosome pathway in a pathophysiologically relevant murine model of reversible heart failure. *J Am Coll Cardiol Basic Trans Science*. 2022;7(12):1214–1228.

**54.** Fang X, Wang H, Han D, et al. Ferroptosis as a target for protection against cardiomyopathy. *Proc Natl Acad Sci U S A*. 2019;116:2672–2680.

**55.** Tanaka R, Umemura M, Narikawa M, et al. Reactive fibrosis precedes doxorubicin-induced heart failure through sterile inflammation. *ESC Heart Fail*. 2020;7:588–603.

**56.** Zhu W, Soonpaa MH, Chen H, et al. Acute doxorubicin cardiotoxicity is associated with p53-induced inhibition of the mammalian target of rapamycin pathway. *Circulation*. 2009;119:99–106.

**57.** Neilan TG, Coelho-Filho OR, Pena-Herrera D, et al. Left ventricular mass in patients with a cardiomyopathy after treatment with anthracyclines. *Am J Cardiol*. 2012;110:1679–1686.

**58.** Lipshultz SE, Colan SD, Gelber RD, Perez-Atayde AR, Sallan SE, Sanders SP. Late cardiac effects of doxorubicin therapy for acute lymphoblastic leukemia in childhood. *N Engl J Med*. 1991;324:808–815.

**59.** Mani K, Javaheri A, Diwan A. Lysosomes mediate benefits of intermittent fasting in cardiometabolic disease: the janitor is the undercover boss. *Compr Physiol*. 2018;8:1639–1667.

**KEY WORDS** anthracycline, apolipoprotein M, autophagy, cardiomyopathy, TFEB

**APPENDIX** For supplemental Methods, tables, and figures, please see the online version of this paper.